

# On the visibility of electron-electron interaction effects in field emission spectra

T. L. Schmidt and A. Komnik

*Physikalisches Institut, Albert-Ludwigs-Universität, D-79104 Freiburg, Germany*

One of the most convenient methods to obtain information about the energy distribution function of electrons in conducting materials is the measurement of the energy resolved current  $j(\omega)$  in field emission (FE) experiments. Its high energy tail  $j_{>}(\omega)$  (above the Fermi edge) contains invaluable information about the nature of the electron-electron interactions inside the emitter. Thus far,  $j_{>}(\omega)$  has been calculated to second order in the tunnelling probability, and it turns out to be divergent toward the Fermi edge for a wide variety of emitters. The extraction of the correlation properties from real experiments can potentially be obscured by the eventually more divergent contributions of higher orders as well as by thermal smearing around  $E_F$ . We present an analysis of both factors and make predictions for the energy window where only the second order tunnelling events dominate the behaviour of  $j_{>}(\omega)$ . We apply our results to the FE from Luttinger liquids and single-wall carbon nanotubes.

PACS numbers: 73.63.Fg; 03.65.Xp; 71.10.Pm

Keywords: A. nanostructures; D. electron-electron interactions; D. tunnelling; E. electron emission spectroscopy

## I. INTRODUCTION

According to the original idea of Fowler and Nordheim<sup>1</sup>, the cold emission of electrons from metallic electrodes can be considered as tunnelling of particles from the conduction band into the vacuum through a triangular barrier. The precise form of the latter is determined by the work function  $W_A$ , by the applied electric field  $F$  as well as by the geometry of the emitter tip, and is characterised by the effective transmission coefficient  $D(\omega)$  for the electrons with energy  $\omega$ <sup>2</sup>. The most important measurable quantities are the energy resolved current  $j(\omega)$  and the total current  $J = \int d\omega j(\omega)$ . The currents drawn from the emitters are usually very small so that  $j(\omega)$  is proportional to the equilibrium energy distribution function of electrons in the vicinity of the tip,  $n_F(\omega)$ , and to  $D(\omega)$ <sup>1</sup>,

$$j(\omega) \sim D(\omega)n_F(\omega). \quad (1)$$

Therefore, at  $T = 0$  no electrons are allowed with energies above the Fermi edge  $E_F$ . However, in 1970, Lea and Gomer succeeded in measuring  $j(\omega)$  to a very high degree of accuracy. They found significant contributions above  $E_F$ <sup>3</sup>. This effect can be attributed to electron-electron interactions inside the emitter. The relevant process is usually referred to as “secondary tunnelling”<sup>2</sup>, during which an electron with energy below the Fermi edge tunnels out of the emitter leaving behind a hot hole. In the second stage, this hole scatters inelastically, producing a secondary electron which can obtain an energy above  $E_F$ . Due to its higher energy, this electron has an increased tunnelling probability and will contribute to a “secondary current”  $j_{>}(\omega)$  above  $E_F$ . Since  $j_{>}(\omega)$  comes about as a result of interactions, its measurement reveals valuable information about the nature of correlations inside the emitter.

Two different types of rigorous calculations of  $j_{>}(\omega)$

have been attempted so far. The approach of<sup>4</sup> used kinetic equations. In<sup>5</sup> the high-energy tails in  $j(\omega)$  were calculated using non-equilibrium perturbation theory in the tunnelling probability. One of the principal predictions is the asymptotic behaviour toward the Fermi edge, which turns out to be divergent. Both approaches take into account only tunnelling processes of lowest order. To the best of our knowledge thus far no investigations of processes of higher orders have been undertaken despite the fact that they can potentially be even more divergent around  $E_F$  and therefore obscure the predicted effects. With this work we would like to address this problem and analyse the influence of higher order tunnelling processes on  $j_{>}(\omega)$ .

Thermal broadening of the Fermi edge can also prevail over the contributions of lowest order, making their measurement difficult if not impossible. While in conventional Fermi liquid systems this broadening is rather simple to estimate, in many interacting systems it has not yet been analysed. One of the most important of these is the universality class of 1D correlated electrons or the so-called Luttinger liquids (LLs), which are e.g. realised in single-wall carbon nanotubes (SWNTs), as has been shown both theoretically and experimentally<sup>6,7,8,9</sup>.

Recently, the advancement in manufacturing enabled the construction of the first flat panel display which employs carbon nanotubes as emitters<sup>10,11</sup>. Refinement and further development of this technology requires detailed knowledge of their emission spectra. This is the reason why it is important to fully understand the field emission properties of SWNTs. Thus far, theoretical activities in this field have been rather moderate. In this work, we would like to analyse the effects of tunnelling processes of higher orders from LLs along with the effects of thermal broadening of the Fermi edge on the high-energy tail of  $j_{>}(\omega)$  and apply the results to FE from SWNTs.

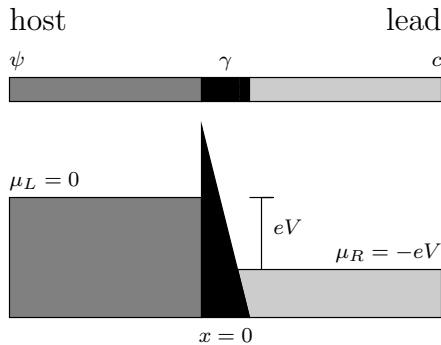


FIG. 1: Schematic view of the system under consideration

## II. NEXT-TO-LEADING ORDER IN TUNNELLING: DIAGRAMMATIC APPROACH

We model the field emission set-up by a heterogeneous tunnelling junction (Fig. 1). The left contact, which will be referred to as “host”, represents the emitter. The chemical potential of this system is set to  $\mu_L = 0$ . We shall assume that tunnelling only takes place precisely at the interface between the conductors. The right contact will be referred to as “lead”, and is represented by a non-interacting Fermi gas with chemical potential  $\mu_R = -eV$ . As during field emission electrons tunnel into vacuum, this potential plays the role of a cut-off and has to be set to the conduction band width or the characteristic energy scale entering  $D(\omega)$ , whichever is larger. The transmission coefficient  $D(\omega)$  of the triangular barrier encountered in field emission depends exponentially on the energy and the work function  $W_A$ . We restrict ourselves to the low temperature limit, where interesting processes will only involve electrons quite close to the Fermi edge. That is why we replace this tunnelling probability by a constant,  $\gamma^2 \sim D(0)$ , where  $\gamma$  is the energy independent tunnelling amplitude (we set  $E_F = 0$  throughout). The model Hamiltonian is then given by

$$H = H[\psi] + H[c] + \gamma[\psi^\dagger(0)c(0) + \psi(0)c^\dagger(0)], \quad (2)$$

consisting of three parts.  $H[\psi]$  and  $H[c]$  are the Hamiltonians of the host and the lead, respectively, and the third term describes the tunnelling events.

Due to the finite applied voltage, the system under consideration is in a non-equilibrium state. The most convenient method of describing such systems is the Keldysh formalism<sup>12</sup>, where we shall be taking  $H_{int} = \gamma[\psi^\dagger(0)c(0) + \psi(0)c^\dagger(0)]$  as the perturbation of the Hamiltonian  $H_0 = H[\psi] + H[c]$ . We shall use the notation employed in<sup>13</sup>, where the Green’s functions are defined by

$$\begin{aligned} g^{--}(t, t') &= -i\langle T[\psi(t)\psi^\dagger(t')]S_C \rangle_0, \\ g^{-+}(t, t') &= i\langle \psi^\dagger(t')\psi(t)S_C \rangle_0, \\ g^{+-}(t, t') &= -i\langle \psi(t)\psi^\dagger(t')S_C \rangle_0, \\ g^{++}(t, t') &= -i\langle \tilde{T}[\psi(t)\psi^\dagger(t')]S_C \rangle_0. \end{aligned} \quad (3)$$

$T$  and  $\tilde{T}$  are time and anti-time ordering operators, respectively, and  $\langle \dots \rangle_0$  stands for the averaging with respect to the ground state of  $H_0$ . We use  $g(t, t')$  to denote Green’s functions of particles in the host, whereas  $G(t, t')$  refers to Green’s functions in the lead. The operator  $S_C$  is defined by the perturbation,

$$S_C = T_C \exp \left\{ -\frac{i\gamma}{\hbar} \int_C dt [\psi^\dagger(t)c(t) + \psi(t)c^\dagger(t)] \right\}. \quad (4)$$

As shown in<sup>14</sup>, the energy resolved current for a certain energy  $\omega > 0$  is proportional to the local Green’s function  $g^{-+}(\omega)$  in the host. Our primary task is to calculate the function  $g^{-+}(\omega)$ . For this purpose we shall perform a perturbative expansion of  $S_C$  in the tunnelling amplitude  $\gamma$ , so that  $g^{-+}(\omega) = g_0^{-+}(\omega) + g_2^{-+}(\omega) + g_4^{-+}(\omega) + \dots$  where  $g_2 \sim \gamma^2$  and  $g_4 \sim \gamma^4$ . As the Fermi edge is still sharp even in interacting systems, the zeroth order does not contribute above  $E_F$ . According to<sup>5</sup>, the second order correction to the Green’s function can be brought to the form,

$$\begin{aligned} g_2^{-+}(\omega) &= \frac{\gamma^2}{\hbar^2} \int dt e^{i\omega t/\hbar} \iint_{-\infty}^{\infty} dt_1 dt_2 \\ &\times \sum_{ij=\pm} (ij) K_{ij}(t, t_1, t_2) G^{ij}(t_1, t_2), \end{aligned} \quad (5)$$

where  $K_{ij}$  are four-point correlators of  $\psi$ -operators which correspond to rectangular diagrams with insertions<sup>14</sup>. It has been shown in<sup>14</sup> that only

$$K_{+-}(t, t_1, t_2) = -\langle \tilde{T}\{\psi^\dagger(0)\psi^\dagger(t_1)\}T\{\psi(t)\psi(t_2)\} \rangle (6)$$

yields a non-zero contribution above  $\omega = 0$ , which diverges toward the Fermi edge.

We can use the same approach that led to (5) and expand to the next-to-leading order in  $\gamma$ . It turns out to be given by

$$\begin{aligned} g_4^{-+}(\omega) &= \frac{i\gamma^4}{2\hbar^4} \int dt e^{i\omega t/\hbar} \iiint_{-\infty}^{\infty} dt_1 \dots dt_4 \\ &\times \sum_{ijkl} K_{ijkl}(t, t_1, t_2, t_3, t_4) G^{ij}(t_1, t_2) G^{kl}(t_3, t_4), \end{aligned} \quad (7)$$

which schematically corresponds to a sum over 16 different hexagon-shaped diagrams, s. Fig. 2, each containing *two* insertions of the lead Green’s functions and a six-point correlator  $K_{ijkl}$  which is similar to the four-point correlators in the second-order case. The structure of the diagrams is not surprising as in this order two successive tunnelling processes are allowed. Since we are only interested in the high-energy contributions above  $E_F$ , we first have to identify the diagrams which may contribute in this situation. As in the case of lowest order contributions, the best way to identify the relevant constellations without explicit calculation is to take advantage of the spectral representation. To that end we have to be able to perform the  $t$ -integration in (7). This

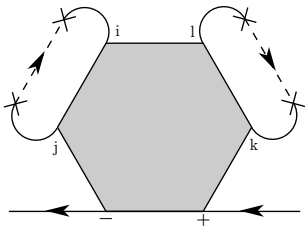


FIG. 2: **Fourth order diagram:** The hexagon corresponds to a six-point correlation function of  $\psi$  operators and the indices  $i, j, k, l = \pm$  denote the respective part of the Keldysh contour. Solid lines depict Green's functions in the host, dashed lines stand for Green's function in the lead wire. Crosses stand for the tunnelling vertices.

can be accomplished by insertion of an appropriate number of complete sets of eigenstates, thereby extracting the  $t$ -dependence.

In order to illustrate the procedure, we shall determine the contribution of the  $K_{----}$  correlation function where the time indices  $t_1$  to  $t_4$  are taken on the time-ordered “-” shoulder of the Keldysh contour. Hence, we wish to calculate

$$g_4^{-+}(\omega) = \frac{i\gamma^4}{4\hbar^4} \int dt e^{i\omega t/\hbar} \iiint dt_1 \cdots dt_4 \quad (8)$$

$$\times \left\langle \psi^\dagger(-t) T[\psi(0) \psi_1^\dagger \psi_2 \psi_3^\dagger \psi_4] \right\rangle_0 \left\langle T[c_1 c_2^\dagger c_3 c_4^\dagger] \right\rangle_0.$$

The time development of the  $\psi(t)$  and  $c(t)$  operators in the interaction picture is governed by the unperturbed Hamiltonians  $H[\psi]$  and  $H[c]$ , respectively. Although due to the interactions in the host, we cannot diagonalise  $H[\psi]$ , we still know that there is a complete set of eigenstates satisfying  $H[\psi]|\nu\rangle = E_\nu|\nu\rangle$  and  $\sum_\nu |\nu\rangle\langle\nu| = 1$  with positive eigenenergies  $E_\nu$ . Inserting a complete set into (8) yields

$$g_4^{-+}(\omega) = \frac{i\gamma^4}{4\hbar^4} \sum_\nu \int dt e^{i\omega t/\hbar} \quad (9)$$

$$\times \langle 0 | e^{-iH[\psi]t/\hbar} \psi^\dagger e^{iH[\psi]t/\hbar} | \nu \rangle A(\nu),$$

where  $A(\nu)$  is independent of  $t$ ,

$$A(\nu) = \iiint dt_1 \cdots dt_4 \quad (10)$$

$$\times \langle \nu | T[\psi(0) \psi_1^\dagger \psi_2 \psi_3^\dagger \psi_4] | 0 \rangle \langle T[c_1 c_2^\dagger c_3 c_4^\dagger] \rangle_0.$$

Hence, the  $t$  integration can be performed and leads to

$$g_4^{-+}(\omega) = \frac{i\gamma^4}{4\hbar^4} \sum_\nu \int dt e^{i\omega t/\hbar} e^{iE_\nu t/\hbar} \langle 0 | \psi^\dagger | \nu \rangle A(\nu)$$

$$= \frac{i\gamma^4}{4\hbar^3} \sum_\nu \delta(\omega + E_\nu) \langle 0 | \psi^\dagger | \nu \rangle A(\nu).$$

As all energies  $E_\nu$  are positive, we conclude that this function does not yield a contribution above  $\omega = 0$ . Similar calculations can be performed for all other correlation functions. We find out, that e.g. in second order, the

only contributing diagram is described by the correlation function,

$$K_{+-} = -\langle \tilde{T}[\psi^\dagger(0) \psi_1^\dagger] T[\psi(t) \psi_2] \rangle, \quad (11)$$

which contributes for  $\omega < eV$ , the upper threshold for second order processes. On the other hand, in fourth order there are only three relevant contributions which are given by

$$K_{+----} = \left\langle \tilde{T}[\psi^\dagger(0) \psi_1^\dagger] T[\psi(t) \psi_2 \psi_3^\dagger \psi_4] \right\rangle_0, \quad (12)$$

$$K_{+--+} = \left\langle \tilde{T}[\psi^\dagger(0) \psi_1^\dagger \psi_3^\dagger] T[\psi(t) \psi_2 \psi_4] \right\rangle_0, \quad (13)$$

$$K_{++++} = \left\langle \tilde{T}[\psi^\dagger(0) \psi_1^\dagger \psi_2 \psi_3^\dagger] T[\psi(t) \psi_4] \right\rangle_0. \quad (14)$$

Two of these correlation functions ( $K_{+----}$  and  $K_{++++}$ ) contribute up to  $\omega = eV$  and have to be counted twice due to reasons of symmetry. The correlation function  $K_{+--+}$  contributes for  $\omega < 2eV$  which is the upper threshold for fourth order processes. In all of these contributions at least one of the insertions is of the type encountered in the lowest order. We know that in the lowest order (the rectangular diagram of<sup>14</sup>) the purely time or anti-time ordered insertions do not lead to contributions above  $\omega = 0$ . Therefore, in the terms where only one of the insertions is of the type  $G^{+-}(\omega)$ , one can regard the corresponding diagram as an effectively rectangular one with respect to high-energy tails.

### III. FIELD EMISSION FROM LUTTINGER LIQUIDS AND SWNTS.

The usual way to proceed after the relevant diagrams have been identified is to perform a perturbative expansion of all contributions in the interaction constant. However, a perturbative breakdown of the six-point correlation functions (hexagons of Fig. 2) in non-equilibrium involves a very large set of diagrams. Performing the same calculation for a LL system does not have that disadvantage. The reason for that is the fact that in the bosonization representation of an LL any possible fermionic correlation function can be computed for any interaction strength without resorting to approximation schemes<sup>15,16,17</sup>. The perturbative results are then expected to be recovered after taking the limit of vanishing interactions. On the other hand, as we are showing later, the results for an LL only have to be slightly modified in order to be applied to the experimentally relevant FE from SWNTs.

Our main goal is the calculation of the kernels  $K_{ijkl}$ . We assume the emitter to be infinite extending from  $x = -\infty$  to  $x = 0$ . Hence, we are dealing with a semi-infinite wire with an open boundary condition (OBC) at its end. Using OBC bosonization<sup>18</sup>, exactly at the emitter tip ( $x = 0$ ), where all tunnelling events take place, we have

for the electron field operator

$$\psi(x=0, t) = \frac{1}{\sqrt{2\pi a}} e^{2\pi i \phi(x=0, t)/\sqrt{g}}, \quad (15)$$

where  $a$  is an infinitesimal cut-off length which can be interpreted as the lattice constant of the underlying lattice model. We omit the ‘‘ladder operator’’ (particle number changing operator) as we are later going to the limit of infinitely long wire  $L \rightarrow \infty$ <sup>17,19</sup>. The bosonic phase field  $\phi$  entering (15) is given by

$$\phi(x=0, t) = \frac{1}{2\pi} \sum_{q>0} \sqrt{\frac{\pi}{Lq}} (e^{-iqvt} a_q + e^{iqvt} a_q^\dagger) e^{-aq/2}. \quad (16)$$

In the above equations,  $g$  is a dimensionless quantity measuring the interaction strength<sup>17</sup>,

$$g = \left(1 + \frac{U_0}{\pi \hbar v_F}\right)^{-1/2}, \quad (17)$$

where  $U_0$  is the Fourier transform of the screened electron-electron interaction potential  $U(x-y)$  at  $q=0$  and  $v_F$  is the Fermi velocity,  $v = v_F/g$ .

By using the Baker-Hausdorff formula, we can calculate arbitrary correlation functions of the type

$$\mathbb{K} = \langle \alpha_1 \cdots \alpha_N \rangle, \quad (18)$$

where  $N$  is an even number and  $\alpha_i$  are fermion creation or annihilation operators,  $\psi^\dagger(t_i)$  or  $\psi(t_i)$ . We arrive at the result,

$$\mathbb{K} = \frac{F(0)^{N/2g}}{\sqrt{(2\pi a)^N}} \left[ \prod_{m=1}^{N-1} \prod_{n=m+1}^N F(t_m - t_n)^{\beta_m \beta_n} \right]^{1/g} \quad (19)$$

where

$$F(t) = 1 - e^{-i\epsilon_0(t-i\delta)}. \quad (20)$$

The parameters  $\epsilon_0$  and  $\delta$  are defined by  $\epsilon_0 = \pi/Lv$  and  $\delta = a/v$ . Furthermore  $\beta_i = +1$  [ $\beta_i = -1$ ] for  $\alpha_i = \psi(t_i)$  [ $\alpha_i = \psi^\dagger(t_i)$ ].

Using (19) and taking into account the time orderings, we obtain for the rectangular diagram<sup>14</sup>

$$\begin{aligned} g_2^{-+}(\omega) &= -\frac{\gamma^2}{(2\pi a \hbar)^2} \int dt e^{i\omega t/\hbar} \iint_{-\infty}^{\infty} dt_1 dt_2 \\ &\times \text{sgn}(-t_1) \text{sgn}(t-t_2) G^{+-}(t_1, t_2) \\ &\times \left[ \frac{F(0)^2 F(-|t_1|) F(|t-t_2|)}{F(-t) F(-t_2) F(t_1-t) F(t_1-t_2)} \right]^{1/g} \end{aligned} \quad (21)$$

Assuming the lead to be a Fermi gas with chemical potential  $\mu_R = -eV$ , the corresponding Green's function becomes

$$G^{+-}(t_1, t_2) = -\frac{\hbar\nu e^{ieV(t_1-t_2)/\hbar}}{2\pi t_1 - t_2 - i\delta}, \quad (22)$$

with an infinitesimal parameter  $\delta$ . For reasons of simplicity, we have assumed a constant density of states  $\nu$  in the lead. Furthermore, we approximate  $F(t)$  by  $F(t) \approx i\epsilon_0(t-i\delta)$ , which is justified for  $L \rightarrow \infty$ . These approximations allow the calculation of  $g_2^{-+}(\omega)$ , which has been performed in<sup>14</sup>. However, the approach of<sup>14</sup> cannot be adapted to the fourth order. Nevertheless, as  $\gamma$  is very small,  $g_4^{-+}(\omega)$  can become important only in the immediate vicinity of the Fermi energy and even that only when it turns out to be more divergent than the lowest order term. Therefore, it is sufficient to find the  $\omega \rightarrow 0$  asymptotics and we require  $eV/\omega \rightarrow \infty$ . In that case, the Green's function  $G^{+-}$  can be shown to become a  $\delta$ -function,

$$G^{+-}(t_1, t_2) \rightarrow -i\hbar\nu\delta(t_1 - t_2). \quad (23)$$

Using this representation, the high energy particle number  $n_2(\omega) = -ig_2^{-+}(\omega)/\hbar$  can readily be calculated and one immediately obtains

$$n_2(\omega) = n_2^c \left( \frac{\omega}{\omega_c} \right)^{1/g-2}, \quad (24)$$

where  $\omega_c = \gamma/a$  and

$$n_2^c = \frac{\nu}{(2\pi)^2} \left( \frac{\gamma}{v\hbar} \right)^{1/g} k_2. \quad (25)$$

$k_2$  contains a numerical prefactor which is given by the dimensionless convergent integral

$$\begin{aligned} k_2 &= (-i)^{1/g} \lim_{\delta \rightarrow 0} \int dy e^{iy} \int_{-\infty}^{\infty} dy_1 \text{sgn}(-y_1) \text{sgn}(y-y_1) \\ &\times \left[ \frac{(-|y_1|)(|y-y_1|)}{(-y-i\delta)(-y_1-i\delta)(y_1-y-i\delta)} \right]^{1/g}. \end{aligned} \quad (26)$$

Within the approximation  $eV/\omega \rightarrow \infty$ , the calculation of the fourth order contributions can be performed likewise. We start with the determination of the contribution of the  $K_{+-+}$  correlator. In analogy with (21), we obtain a similar expression but with two insertions. According to (23) we obtain two  $\delta$  functions which allow to perform two of the four integrations. Switching to dimensionless quantities, we obtain

$$g_4^{-+}(\omega) = \frac{i\hbar\nu}{(2\pi)^3} \frac{\nu\gamma}{2} k_4' \left( \frac{\gamma}{v\hbar} \right)^{1/g} \left( \frac{\gamma}{a\omega} \right)^{3-1/g}, \quad (27)$$

where the numerical factor  $k_4'$  is given by

$$\begin{aligned} k_4' &= (-i)^{1/g} \int dy e^{iy} \iint dy_1 dy_3 \\ &\times \frac{\text{sgn}(-y_1) \text{sgn}(-y_3) \text{sgn}(y-y_1) \text{sgn}(y-y_3)}{(-y-i\delta)^{1/g}} \\ &\times \left[ \frac{-|y_1||y_3||y_1-y_3|}{(-y_1-i\tilde{\delta})(-y_3-i\tilde{\delta})(y_1-y-i\tilde{\delta})} \right]^{1/g} \\ &\times \left[ \frac{|y-y_1||y-y_3||y_1-y_3|}{(y_1-y_3-i\tilde{\delta})(y_3-y-i\tilde{\delta})(y_3-y_1-i\tilde{\delta})} \right]^{1/g}. \end{aligned} \quad (28)$$

The other diagrams,  $(ijkl) = (+---)$  and  $(ijkl) = (++++)$ , can be treated in the same way with the exception that the time ordering combinatorics is significantly more complicated. However, we found that all three diagrams yield the same leading power-law energy dependence,

$$n_4(\omega) = n_4^c \left( \frac{\omega}{\omega_c} \right)^{1/g-3}, \quad (29)$$

with

$$n_4^c = \frac{\nu}{(2\pi)^3} \frac{\nu\gamma}{2} \left( \frac{\gamma}{v\hbar} \right)^{1/g} k_4. \quad (30)$$

For the  $(ijkl) = (+-+-)$  case the corresponding  $k_4'$  is given by (28). Numerical evaluation of  $k_4'$  yields a value around unity. Due to the different time ordering combinatorics of the six-point correlation functions, the numerical prefactors  $k_4''$  and  $k_4'''$  for the other two diagrams cannot be written in a compact form similar to (28). As the other two diagrams are related to those of the second order in tunnelling (see Section II),  $k_4''$  and  $k_4'''$  have to be of the same order of magnitude as  $k_4'$ .

Equation (29) is the central result of this paper. The contribution of next-to-leading order processes turns out to be even more divergent than the leading order in case of weak interactions,  $g > 1/2$ . However, we expect the overall prefactor to be negative as in the fourth order in tunnelling the recombination of the secondary holes and secondary electrons, stemming from different primary processes, is allowed, effectively suppressing the high-energy tails in  $j_>(\omega)$ . Taking the limit  $g \rightarrow 1$  we expect to obtain the asymptotics of the next-to-leading term for a Fermi liquid,  $n_4(\omega) \sim 1/\omega^2$ . Similarly to the leading order tunnelling results, at  $g = 1$   $j_>(\omega)$  is identically zero due to a vanishing prefactor  $k_4$ . That can be shown analytically.

So far, all calculations have been made for the case of a spinless Luttinger liquid. However, carbon nanotubes are known to be described in terms of a four-channel LL<sup>6,7,20</sup>. The four channels are responsible for the charge-flavour ( $\phi_{c-}$ ), total spin ( $\phi_{s-}$ ), spin-flavour ( $\phi_{s+}$ ) and total charge ( $\phi_{c+}$ ) excitations. The three former are non-interacting ( $g = 1$ ) whereas the latter possesses the Luttinger parameter  $g_{c+} = (1 + 4\tilde{V}_0/\pi\hbar v_F)^{-1/2}$ , where  $\tilde{V}_0$  is the  $k = 0$  component of the Fourier transform of the screened interaction potential. It can further be shown that the field operator  $\psi$  can be written in terms of Bose fields as

$$\psi = \frac{1}{2\pi a} \exp \left[ \pi i (\phi_{c+}/\sqrt{g_{c+}} + \phi_{c-} + \phi_{s+} + \phi_{s-}) \right]. \quad (31)$$

As different species of  $\phi$  operators commute, all correlation functions factorise. Therefore, the results for the one-channel LL can be applied to SWNTs by the simple replacement

$$g^{-1} \rightarrow \frac{g_{c+}^{-1} + 3}{4}. \quad (32)$$

An estimation of the typical interaction parameter  $g$  can be done using the following formula, which relates the geometry of the nanotube to the interaction constant  $g_{c+}$ <sup>20</sup>,

$$g_{c+} = \left( 1 + \frac{8e^2}{\pi\kappa\hbar v_F} [\ln(L/2\pi R) + 0.51] \right)^{-1/2}, \quad (33)$$

where  $\kappa$  is the dielectric constant,  $L$  is the length of the nanotube and  $R$  its radius. Assuming typical values we arrive at an interaction constant  $g_{c+} \approx 0.2$  which leads to an effective  $g \approx 0.5$ .

#### IV. VISIBILITY OF HIGH ENERGY TAILS

Thus far, we have discussed the zero temperature case, where a non-trivial high-energy tail in the energy resolved current is produced by the interaction effects. However, such a tail can trivially emerge as a result of the thermal broadening of the Fermi edge. In this Section, we shall address the problem of distinguishing the correlation effects from those of finite temperature restricting ourselves to the model of spinless LL.

We first calculate the width of the broadening as a function of interaction constant and temperature. Obviously, the main contribution to  $j_>(\omega)$  simply stems from the zeroth order particle density for a Luttinger liquid, which can be brought to the form<sup>21</sup>

$$n_T(\omega) = \frac{1}{\hbar a} \int_{-\infty}^{\infty} dt e^{i\omega t/\hbar} \frac{\sin^\lambda \left( \frac{\pi a}{\hbar\beta v} \right)}{\sin^\lambda \left[ \frac{\pi}{\hbar\beta v} (-i\omega t + a) \right]}, \quad (34)$$

where  $\lambda = 1/g$ . In order to perform this integral, it is convenient to express the sine function in the denominator as an exponential and to rewrite the exponent  $\lambda$  in the denominator with the help of the binomial formula. Then, the integral can be performed and we obtain a representation of  $n(\omega)$  in terms of the hypergeometric function  $F$ <sup>22</sup>,

$$n_T(\omega) = \frac{\sin^\lambda \left( \frac{\pi a}{\hbar\beta v} \right) (2i)^\lambda}{\hbar a} [I_\lambda(\omega) + (-1)^\lambda I_\lambda^*(\omega)] \quad (35)$$

with

$$I_\lambda(\omega) = \frac{\hbar\beta}{\pi\lambda - i\beta\omega} \times F \left( \lambda, \frac{\lambda}{2} - \frac{i\beta\omega}{2\pi}, 1 + \frac{\lambda}{2} - \frac{i\beta\omega}{2\pi}, e^{-2\pi i a/(\hbar\beta v)} \right). \quad (36)$$

This function only depends on the combination  $\beta\omega$  rather than on  $\omega$  alone. Consequently, we can deduce that the width of the thermal broadening will be of the form  $\omega_C = k_B T f(\lambda)$  with a function  $f(\lambda)$  independent of the temperature.

Using an appropriate expression for the hypergeometric function in the case  $\lambda = 1$  and using the expansion for  $a \rightarrow 0$ , the Fermi distribution function of the

non-interacting case can easily be recovered. For the interacting case, i.e. for  $\lambda > 1$ , we need the following expansion<sup>22</sup>,

$$F(x, y, z, e^{i\varphi}) \approx \frac{\Gamma(z)\Gamma(x+y-z)}{\Gamma(x)\Gamma(y)} \quad (37)$$

$$\times (1 - e^{i\varphi})^{z-x-y} [1 + O(e^{i\varphi} - 1)]$$

$$+ \frac{\Gamma(z)\Gamma(z-x-y)}{\Gamma(z-x)\Gamma(z-y)} [1 + O(e^{i\varphi} - 1)].$$

Neglecting terms of order  $O(e^{i\varphi} - 1)$  which is appropriate in the limit of small  $a$ , after some algebraic transformations we arrive at

$$n_T(\omega) = \frac{1}{\hbar v} \left( \frac{2\pi a}{\hbar\beta v} \right)^{\lambda-1} \Gamma(1-\lambda) \sin(\pi\lambda) \quad (38)$$

$$\times \frac{e^{-\beta\omega/2}}{[\cosh(\beta\omega) - \cos(\pi\lambda)] \left| \Gamma(1 - \frac{\lambda}{2} - \frac{i\beta\omega}{2\pi}) \right|^2}.$$

Having established this relation for finite temperatures, we can estimate the visibility of the second order processes by comparing its contribution  $n_2(\omega)$  to the contribution  $n_T(\omega)$ . The result is

$$\frac{n_2(\omega)}{n_T(\omega)} = \frac{1}{(2\pi)^{1/g+1}} \left( \frac{\nu\gamma^2\beta}{a} \right) \frac{k_2[\cosh(\beta\omega) - \cos(\pi/g)]}{\Gamma(1-1/g)\sin(\pi/g)} \quad (39)$$

$$\times (\beta\omega)^{1/g-2} \left| \Gamma(1 - \frac{\lambda}{2} - \frac{i\beta\omega}{2\pi}) \right|^2 e^{\beta\omega/2}.$$

In order to eliminate the tunnelling amplitude  $\gamma$  we can use the following relation with the total current  $I$  and the voltage  $V$ <sup>2,23</sup>,

$$I = g\Gamma(1-1/g)\sin(\pi/g) \frac{e\gamma^2\nu}{2\pi^2\hbar a} \left( \frac{aeV}{\hbar v} \right)^{1/g}. \quad (40)$$

Using this equation, we arrive at the following result

$$\frac{n_2(\omega)}{n_T(\omega)} = \kappa f_0(\beta, I, V) f_1(\beta\omega), \quad (41)$$

where

$$\kappa = \frac{(2\pi)^{1-1/g} k_2}{2g\Gamma^2(1-1/g)\sin^2(\pi/g)}, \quad (42)$$

$$f_0(\beta, I, V) = \frac{\hbar\beta I}{e} \left( \frac{\hbar v}{aeV} \right)^{1/g}, \quad (43)$$

$$f_1(\beta\omega) = [\cosh(\beta\omega) - \cos(\pi/g)] (\beta\omega)^{1/g-2} \quad (44)$$

$$\times \left| \Gamma\left(1 - \frac{1}{2g} - \frac{i\beta\omega}{2\pi}\right) \right|^2 e^{\beta\omega/2}.$$

Additionally, we can determine the ratio of the second and fourth order tunnelling. Using (24) and (29), one obtains

$$\frac{n_2(\omega)}{n_4(\omega)} = \frac{2g}{\pi} \Gamma(1-1/g)\sin(\pi/g) \frac{k_2}{k_4} \left( \frac{aeV}{\hbar v} \right)^{1/g} \frac{e\omega}{I\hbar}. \quad (45)$$

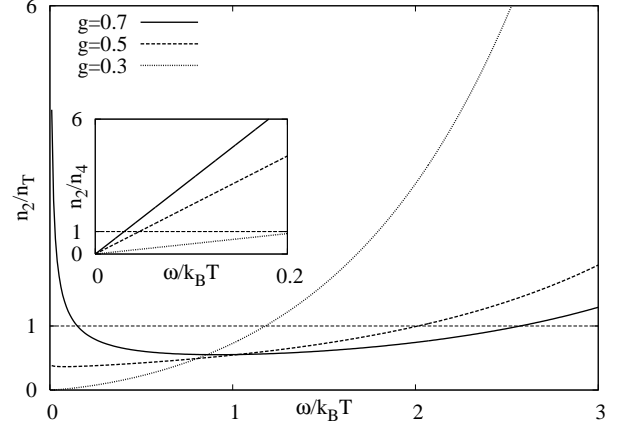


FIG. 3: Ratio of the secondary current to thermal broadening. In the inset: Ratio of the second order to the fourth order contribution

In order to access information about the nature of correlations inside the host it is sufficient to compare the experimental data to the results in the lowest order in tunnelling, as the latter constitute the dominant contributions and are known in great detail. However, they are the more pronounced the closer to  $E_F$   $j_>(\omega)$  is measured. In these regions the influence of both  $n_4$  and  $n_T$  becomes important. Therefore, from the experimental point of view it is very important to possess detailed information about the energy window where only  $n_2$  yields the major contribution. Having established the relations (45) and (39) between all three principal contributions to the high-energy tails we are now in a position to accomplish this task.

The lower threshold of experimentally measurable currents is expected to be about 1nA. Experimentally applicable electric fields are in the range of 1V/ $\mu\text{m}$  and the interface width is of the order of magnitude of 1nm. Taking into account the amplification factor due to the sharpness of the emitter tip of  $\sim 10^3$  we estimate the cut-off parameter  $V$  to be around 1V. Assuming the experiment to be performed at  $T = 1\text{K}$ , the resulting graphs for the ratios of  $n_2(\omega)$  to  $n_T(\omega)$  and  $n_2(\omega)$  to  $n_4(\omega)$  are presented in Fig. 3. In order to compare the energy scales, we note that at a temperature of 1K and a current of 1nA,  $k_B T \approx 20I\hbar/e$ . With our choice of parameters, we arrive at the following values for the lower thresholds for  $g \approx 0.5$ :  $n_2 > n_T$  for  $\omega > 2k_B T$ , and  $n_2 > n_4$  for  $\omega > 0.05k_B T$ , so that at least at 1K the processes of higher order in tunnelling can safely be neglected. The lower threshold for  $j_>(\omega)$  is then of the order of temperature. The upper threshold for the second order in tunnelling is given by  $\omega = eV$  as pointed out in Section II.

## V. CONCLUSIONS

We have investigated field emission from strongly correlated emitters with special focus on the high-energy tails of the energy resolved current. Using Keldysh diagram technique, we could isolate the relevant diagrams in fourth order in the tunnelling amplitude. Modelling the interaction in the host wire by a Luttinger liquid with an interaction parameter  $g$  we could reproduce the already known leading asymptotics of the second order result,  $j_{>} \sim \omega^{1/g-2}$  by an alternative approach. Using this method we succeeded in identifying the leading behaviour of the high-energy tails in fourth order in the tunnelling amplitude, which turns out to be given by  $\omega^{1/g-3}$ . Furthermore, we addressed the question of the observability of the secondary current by comparing the

second order in tunnelling amplitude contribution with the broadening of the Fermi edge at finite temperatures as well as with the fourth order contribution. With typical parameter values at hand we made an estimation of the energy window where only tunnelling processes of second order give dominant contributions to the particle energy distribution above the Fermi edge.

## Acknowledgments

The authors would like to thank A. O. Gogolin and H. Grabert for many inspiring discussions. This work was supported by the Landesstiftung Baden–Württemberg gGmbH (Germany) and by the EC network DIENOW.

- 
- <sup>1</sup> R. Fowler and L. Nordheim, Proc. Roy. Soc. London, Ser. A **119**, 173 (1928).  
<sup>2</sup> J. Gadzuk and E. Plummer, Rev. Mod. Phys. **45**(3), 487 (1973).  
<sup>3</sup> C. Lea and R. Gomer, Phys. Rev. Lett. **25**(12), 804 (1970).  
<sup>4</sup> J. W. Gadzuk and E. W. Plummer, Phys. Rev. Lett. **26**, 92 (1971).  
<sup>5</sup> A. Komnik and A. O. Gogolin, Phys. Rev. Lett. **87**, 256806 (2001).  
<sup>6</sup> R. Egger and A. Gogolin, Phys. Rev. Lett. **79**, 5082 (1997).  
<sup>7</sup> C. Kane, L. Balents, and M. Fisher, Phys. Rev. Lett. **79**, 5086 (1997).  
<sup>8</sup> M. Bockrath, D. H. Cobden, J. Lu, A. G. Rinzler, R. E. Smalley, L. Balents, and P. L. McEuen, Nature **397**, 598 (1999).  
<sup>9</sup> Z. Yao, H. W. C. Postma, L. Balents, and C. Dekker, Nature **402**, 273 (1999).  
<sup>10</sup> S. Fan, Science **283**, 512 (1999).  
<sup>11</sup> W. Choi, Appl. Phys. Lett. **75**(20), 3129 (1999).  
<sup>12</sup> L. V. Keldysh, Zh. Eksp. Teor. Fiz. **47**, 1515 (1964).  
<sup>13</sup> L. Landau and E. Lifshitz, *Quantum Mechanics* (Pergamon, Oxford, 1982).  
<sup>14</sup> A. Komnik and A. Gogolin, Phys. Rev. B **66**, 035407 (2002).  
<sup>15</sup> J. Luttinger, J. Math. Phys. **4**, 1154 (1963).  
<sup>16</sup> S. Tomonaga, Prog. Theor. Phys. **5**, 544 (1950).  
<sup>17</sup> F. Haldane, J. Phys. C **14**, 2585 (1981).  
<sup>18</sup> M. Fabrizio and A. Gogolin, Phys. Rev. B **51**(24), 17827 (1995).  
<sup>19</sup> H. Grabert, in S. Sarkar, ed., *Exotic States in Quantum Nanostructures* (Kluwer, 2002), cond-mat/0107175.  
<sup>20</sup> R. Egger and A. Gogolin, Eur. Phys. J. B **3**, 281 (1997).  
<sup>21</sup> J. v. Delft and H. Schoeller, Ann. Phys. (Leipzig) **4**, 225 (1998), cond-mat/9805275.  
<sup>22</sup> M. Abramowitz and I. Stegun, *Handbook of Mathematical Functions* (National Bureau of Standards, 1964).  
<sup>23</sup> T. L. Schmidt, *Field emission from strongly correlated wires*, diploma thesis, Albert-Ludwigs-Universität Freiburg (2004).